BI-DIRECTIONAL REFLECTANCE DISTRIBUTION FUNCTIONS (BRDF) OF BENTHIC SURFACES IN THE LITTORAL ZONE

Kenneth J. Voss, Hao Zhang, and Al Chapin
Department of Physics
University of Miami
Coral Gables, Fl. 33124
(305)284 2323
voss@physics.miami.edu

The bi-directional reflectance distribution function (BRDF) describes the angular distribution of reflectance for any angle of light incident on a surface. It is a crucial parameter for modeling the light field near the benthic surface, and is important for understanding the remote sensing signal from shallow waters. We have been making measurements of this parameter for varied benthic surfaces in the Bahamas during the ONR sponsored Coastal Benthic Optical Properties experiment (CoBOP) for the last several years. While this parameter is generally assumed to be Lambertian, meaning that the radiance reflected from the surface does not depend on viewing angle, we have found that in general this is not the case. Even simple surfaces, such as sand, exhibit non-Lambertian behavior in two directions. The first is in the specular direction, where there can be a small enhancement in the reflectance for many natural surfaces. The largest non-Lambertian feature seems to be in the "hotspot" or backward direction. In almost all the samples we have seen, for an incident illumination polar angle(θ_i)>25°, there is an enhancement of the reflectance in the hotspot.

The instrument we have used to make these measurements is described in detail elsewhere.[1] The main feature is that it can make in-situ measurements of the bi-directional reflectance in a manner which is suitable for diver operation. The data we show in this paper is more properly the reflectance factor (REFF).[2] This is related to the BRDF by:

$$REFF(\theta_i, \theta_v, \phi) = \pi \, BRDF(\theta_i, \theta_v, \phi)$$

The REFF for a uniform 100% Lambertian reflector would be 1.0 everywhere. Thus the REFF shows the deviation from a Lambertian reflector in a simple, obvious, and quantitative manner.

As discussed above we find that the BRDF (and REFF) of natural surfaces deviates from a Lambertian surface most strongly in the “hotspot” direction. The function we have chosen to fit our data is the following:

For θ_i <25° :

$$REFF(\theta_i, \theta_v, \phi) = A*\theta_v^2 + B*\cos(\phi)*\theta_v + C$$

For θ_i >25° :

$$REFF(\theta_i, \theta_v, \phi) = A*\theta_v^2 + B*\cos(\phi)*\theta_v + C + \{W0 + W1*\exp(-W2\,\gamma)\}$$

$$A(\theta_i) = K1A + K2A * \theta_i + K3A * \theta_i^2$$

$$B(\theta_i) = K1B + K2B * \theta_i + K3B * \theta_i^2$$

$$C(\theta_i) = K1C + K2C * \theta_i + K3C * \theta_i^2$$

$$Wo(\theta_i) = K1W0 + K2W0 * \theta_i + K3W0 * \theta_i^2$$

$$W1(\theta_i) = K1W1 + K2W1 * \theta_i + K3W1 * \theta_i^2$$

$$W2(\theta_i) = K1W2 + K2W2 * \theta_i + K3W2 * \theta_i^2$$

Where θ_v is the polar view angle, θ_i is the polar incident angle, ϕ is the azimuthal view angle ($\phi = 0$ corresponds to back scattering), and γ is the phase angle between the incident and scattered beam ($\gamma = 0$ for direct back scattering). K1, K2, and K3 are the corresponding terms for A, B, etc. described in Tables 1 and 2. All angles are in degrees. The function, for $\theta_i < 25°$, corresponds to a simple function described by Walthall et al.[3] The hotspot only seems to become important at $\theta_i > 25°$. At these angles we add in a simple exponential function dependent on the phase angle between the scattered and incident light as shown above. The parameters for two of our samples are shown in Tables 1 and 2. These two samples are for Yellow Grapestone, a sample from the area of Normans Pond outflow, near Lee Stocking Island, and a brightwhite sand area. These are

Table 1) Yellow Grapestone

Color		**A**	**B**	**C**	**W0**	**W1**	**W2**
Red 658 nm	K1	-9.611e-06	-4.301e-06	2.370e-01	3.279e-03	-1.359e-01	0.05692
	K2	6.0730e-08	2.018e-05	1.945e-05	2.680e-04	7.415e-03	
	K3	3.419e-09		-2.691e-05			
Green 570 nm	K1	-8.158e-06	-6.725e-05	2.531e-01	5.483e-03	-1.307e-01	0.0534
	K2	-1.384e-07	1.930e-05	2.308e-04	1.754e-04	7.398e-03	
	K3	7.331e-09		-3.128e-05			
Blue 475 nm	K1	-7.838e-06	-1.108e-05	1.354e-01	2.806e-04	-7.714e-02	0.061
	K2	1.015e-07	1.184e-05	2.369e-05	1.844e-04	4.761e-03	
	K3	1.508e-09		-1.673e-05			

Table 2) White Sand

Color		A	B	C	W0	W1	W2
Red 658 nm	K1	1.598e-06	9.242e-06	5.099e-01	7.562e-03	-1.335e-01	0.1027
	K2	3.028e-08	2.017e-05	1.560e-03	5.945e-04	6.233e-03	
	K3	3.536e-09		-3.557e-05			
Green 570 nm	K1	8.430e-06	-2.840e-04	5.110e-01	-1.678e-03	-8.925e-02	0.07769
	K2	-3.672e-07	2.070e-05	-4.462e-05	6.653e-04	5.762e-03	
	K3	9.871e-09		-1.627e-05			
Blue 475 nm	K1	-6.200e-07	-2.410e-05	4.330e-01	4.113e-06	-1.535e-01	0.07288
	K2	5.665e-08	1.867e-05	9.749oe-04	4.602e-04	7.747e-03	
	K3	3.591e-09		-2.771e-05			

both submerged samples. The Yellow Grapestone sample has larger effective grainsize, was heavily impacted by a biofilm, and was distinctively colored due to the biofilm. The white sand was very clean, and appeared very bright and white. These two samples are chosen as examples of our data. More samples and more information on grain sizes, etc. will be discussed in a later paper.

As an example of how well this model works, we will show examples of these two samples, at two incident angles (0° and 65°) and one color (red = 658 nm). In these figures the polar angle is linearly proportional to the distance from the center of the graph. The center of the graph represents $\theta_v = 0°$. The specular (forward scattering) direction is towards the bottom of these graphs. The hotspot (backscattering) direction is towards the top of the graphs. The crosses in Figure 1(A) are where our viewing angles are, which shows where the measurements the contours are built upon exist. Contours are at 0.02 steps. The Figures on the left (A, C, and E) are for $\theta_i = 0°$, while those on the right (B, D, and F) are for $\theta_i = 65°$ incident angle. The top row are the measured REFF's. The second row is the modeled REFF, using the coefficients in the Table 1 and the equations displayed above. The last row is the difference, ABS(Model-Measured), between the two.

The first sample (Figure 1) is for Yellow Grapestone. In this sample the $\theta_i = 0°$ measurements show an REFF that is approximately Lambertian, but does fall off a little towards the edge. As can be seen in Figure 1E, the modeled REFF fits the measurements very well, within 0.04 everywhere in the field. For this angle there is neither a hotspot in

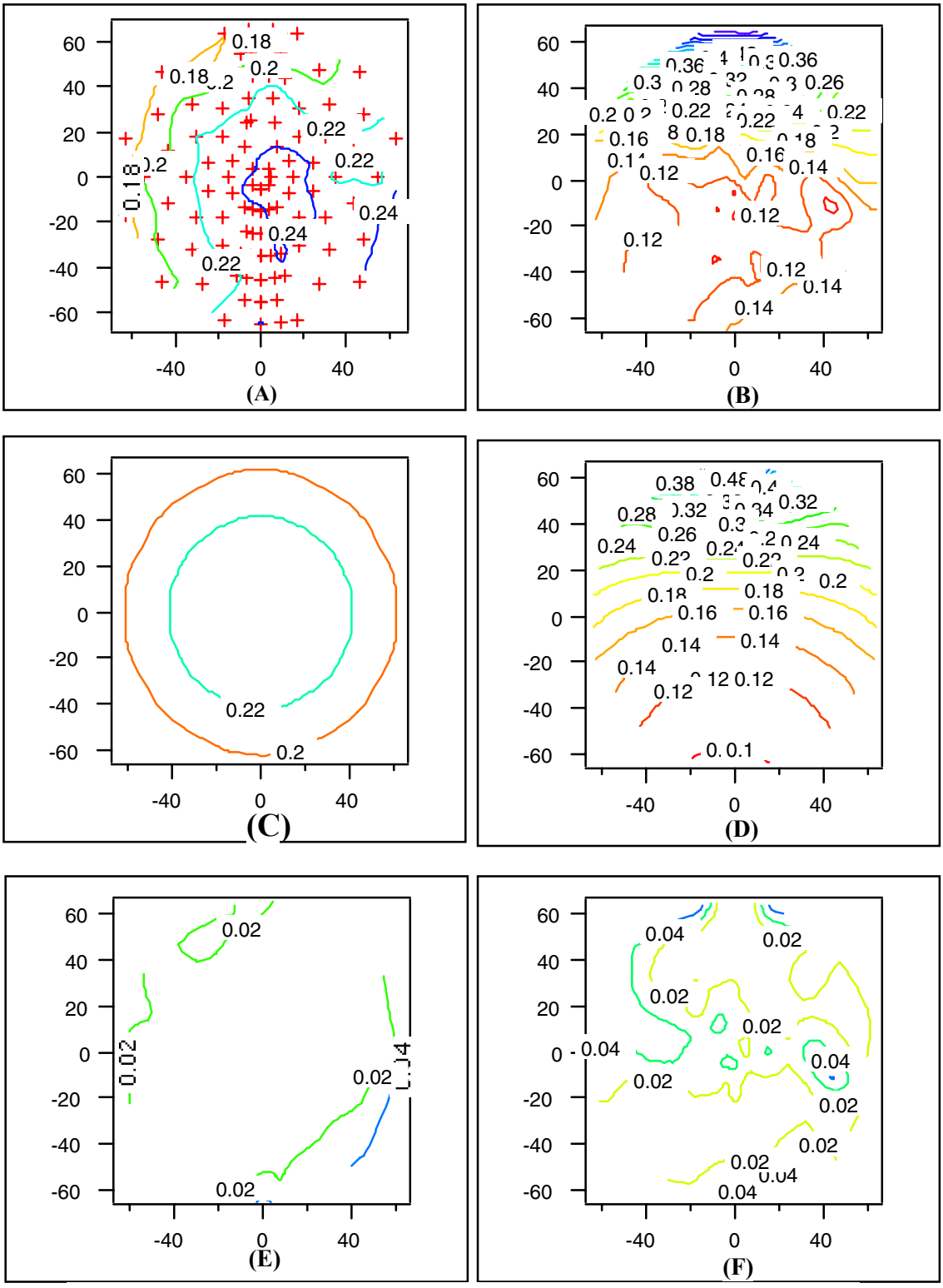

Figure 1) Yellow Grapestone, 658nm. (A) Measured REFF, θ_i=0°. (B) Measured REFF θ_i=65°. (C) Model REFF, θ_i=0°. (D) Model REFF, θ_i=65°. (E) ABS (Model - Measured) REFF, θ_i=0°. (F) ABS (Modeled - Measured) REFF, θ_i=65°

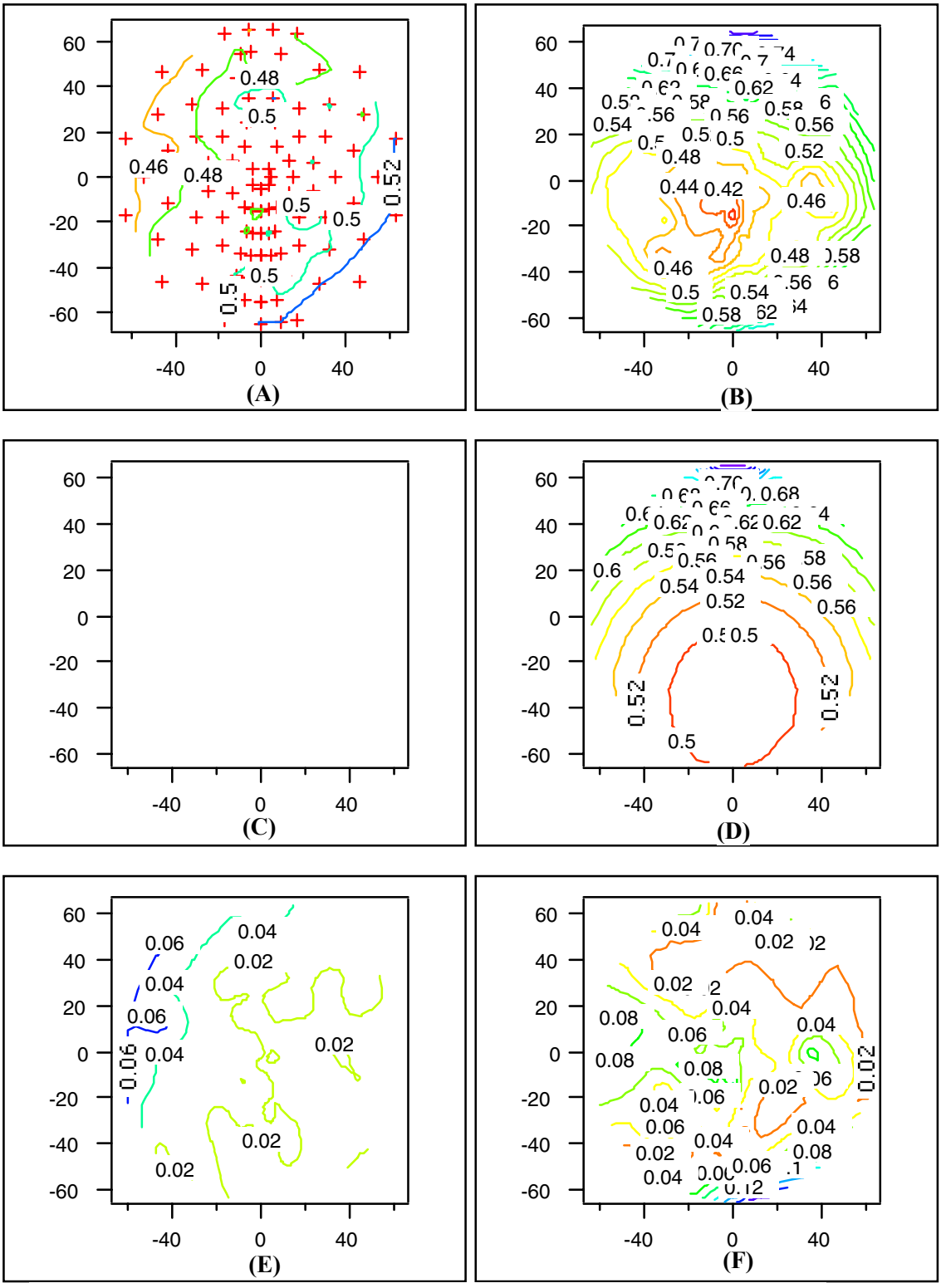

Figure 2) White Sand Sample, 658nm. (A) Measured REFF, θ_i=0°. (B) Measured REFF θ_i=65°. (C) Model REFF, θ_i=0°. (D) Model REFF, θ_i=65°. (E) ABS (Model - Measured) REFF, θ_i=0°. (F) ABS (Modeled - Measured) REFF, θ_i=65°

the data or in the model. For the θ_i =65° measurements, there is a strong hotspot (a factor of 3 or more enhancement). As can be seen in Figure 1F, the modeled hotspot does a very good job of reproducing the measured data. Once again the model fits the data within 0.04.

Figure 2 shows the data for the red channel (658nm) for a white sand sample. In this case for θ_i =0°, the sample is very lambertian over the whole image. In fact the model fit does not have any contours in the image, yet fits the data within 0.04 or so. For θ_i =65° the hotspot again appears, but to less of an extent then the Yellow Grapestone (only a factor of 2 enhancement). The model again fits the hotspot well, but note the specular direction. In the data there was a specular peak to the data, which is not represented in our model. This shows up explicitly in the difference graph (Figure 2F) where the difference reaches over 0.12. At this time we do not have a functional fit for the specular direction, because most of our samples have not required it. This points out that in specific cases a specular component does exist and we will need to improve our fit to include this component. However even here our existing model fits the measured reflectance within 20% of the nadir reflectance.

These two examples show where we are in our efforts. We will soon be looking at various aspects, such as physical parameters of the sediment (Grain size, porosity) to look at the variations in the BRDF between samples. We are currently working on a longer publication which will include more of the measured samples, with the parameters of the relevant analytical fit.

REFERENCES

1. K. J. Voss, A. Chapin, M. Monti, and H. Zhang, “An instrument to measure the Bi-directional reflectance distribution function (BRDF) of surfaces”, submitted to Applied Optics, 2000.

2. B. Hapke, “Theory of reflectance and emittance spectroscopy, Topics in remote sensing Vol. 3”, Cambridge University Press, New York, 1993.

3. C. L. Walthall, J. M. Norman, J. M Welles, G. Cambell, and B. L. Blad, “Simple equation to approximate the bidirectional reflectance from vegetative canopies and bare soil surfaces”, Applied Optics, 24, 383 – 387, 1985.